ON THE CHARACTER AND CATALYTIC ACTIVITY OF DEFECTS FORMED BY γ-IRRADIATION OF H- AND AlH-ZEOLITES

B. WICHTERLOVÁ[a], S. Beran[a], J. Nováková[a] and Z. Prašil[b]

J. Heyrovský Institute of Physical Chemistry and Electrochemistry, Czechoslovak Academy of Sciences, CS-121 38 Prague, Czechoslovakia (a)

Institute for Research, Production and Applications of Radioisotopes, CS-102 27 Prague, Czechoslovakia (b)

ABSTRACT

It has been found that various defects are formed by the γ-irradiation of zeolites, depending on the type of the original zeolite. With the HY and HZSM-5 zeolites, skeletal defects consist of an electron hole on a skeletal oxygen atom sharing one Si and one Al skeletal atom (Si-Ȯ-Al), as well as an electron hole delocalized on several skeletal oxygens $(-O-)_n^{\cdot}$. With the AlHY and Al_xO_yHZSM-5 zeolites containing extralattice Al, electron holes on oxygen atoms neighbouring two Al atoms (Al-Ȯ-Al defects), along with some delocalized $(-O-)_n^{\cdot}$ defects, have been detected. These conclusions are based on the ESR spectra measurements and on model quantum chemical calculations. A considerable activity of the γ-irradiated zeolites in the D_2-H_2 exchange was observed at room temperature. While the skeletal Si-Ȯ-Al and $(-O-)_n^{\cdot}$ defects are quenched by hydrogen, the Al-Ȯ-Al defects are rather stable. For this reason the γ-irradiated zeolites containing extralattice Al exhibit higher and very stable activity in the D_2-H_2 isotopic exchange compared to H-zeolites.

INTRODUCTION

Since the appearance of the first paper by Stamires and Turkevich dealing with the paramagnetic resonance absorption of γ-irradiated zeolites (1), the structure of the defects formed has been studied in detail (2-6). A positive effect of the irradiation on zeolite catalytic activity in the cracking reaction and CO_2 methanation has also been observed (7,8).

EPR studies have shown that the low temperature γ-irradiation of HY zeolites is connected with the formation of V center type defects and that the ejected electrons are trapped either by H^+ ions (creating H atoms entrapped within zeolite structure) or in the insulator material (5). The V center represents an electron hole localized in lone pair orbitals of skeletal oxygen atoms sharing two skeletal silicon atoms and/or one silicon and one aluminum skeletal atom. The stability of the centers is assumed to be strongly dependent on the electron scavengers. An electron hole lo-

cated on an oxygen atom sharing two aluminum atoms in stabilized Y as well as AlHY zeolites was detected (2,3). This result was taken as evidence that stabilized zeolites contain some dimers of aluminum species which have never been observed in pure γ-irradiated γ- and η-alumina.

Because of a complete lack of the data in literature on the relationship between the structure of defects in irradiated zeolites and their stability and reactivity this problem is considered here by studying various defects in H- and Al-Y and ZSM zeolites. For these purposes ESR spectroscopy, quantum chemical model calculations and measurements of catalytic activity in D_2-H_2 exchange were employed.

EXPERIMENTAL

The starting NH_4Y (70 % of exchange) and ZSM-5 zeolites were supplied by the Institute for Oil and Hydrocarbon Gases, Czechoslovakia. Prior to the ionic exchange of the ZSM-5 zeolite with 0.5 m HNO_3 at 298 K for 24 hours (HZSM-5), the zeolite was calcinated in an oxygen stream at 870 K for 6 hours. Extralattice Al was introduced into the HZSM-5 zeolite cavities by supporting an $Al(NO_3)_3$ solution followed by the zeolite calcination in an oxygen stream at 770 K for 5 hours. Extralattice Al was incorporated into the NH_4Y zeolite by ion exchange with 0.1 m $AlCl_3$ solution at pH 4 at 360 K. The composition of the zeolites was determined by AAS after disolution of the samples (Table 1).

Table 1

Composition and Ar sorption capacity of zeolites

irradiated zeolite	Si/Al total	Si/Al latt.	sorption capacity[*] (Ar, mmol/g)	
			prior irr.	after irr.
HY	2.17	2.17	10.7	10.6
AlHY	1.86	2.17	9.6	9.7
HZSM-5	13.6	13.6	5.3	5.5
Al_xO_yHZSM-5	5.08	13.6	5.2	5.1

[*]Sorption capacity ($1.33 \cdot 10^4$ Pa of Ar at 80 K) was measured on samples evacuated at 670 K and related to 1 g of dry zeolite

The preservation of the zeolite structures after the introduction of extralattice Al as well as after the zeolite irradiation was controlled by testing the sorption capacity for argon (see Table 1) and using the IR spectra of skeletal vibrations. Before irradiation the zeolites (placed in an EPR tube and/or in a reactor) were treated in a vacuum of 10^{-3} Pa at a temperature of 670 K and sealed off. The ESR spectra and the reactivity of the zeolites were measured immediately after the γ-irradiation without exposure to the air.

The γ-irradiation of zeolites was performed at 298 K in a ^{60}Co cell for doses of about 10^5Gy. The X-band ESR spectra were recorded at 80 K on an ERS-220 spectrometer (Academy of Sciences, Berlin) with a modulation frequency of 100 kHz. The magnetic field was measured by proton magnetometer related to a Mn^{2+} standard.

The catalytic activity of the irradiated zeolites was tested by measuring the rate of isotopic exchange of the mixture of D_2 and H_2 molecules at room temperature. The irradiated zeolite (0.1 g) was allowed to react with 2×10^2 Pa of hydrogen isotopes in a static apparatus (volume, 700 cm^3). A negligible amount of gases was linked directly to a mass spectrometer (MCH 1302, USSR). No exchange between the gaseous deuterium and the zeolitic OH groups was observed at this temperature. The exchange rate R (atoms $g^{-1}min^{-1}$) was evaluated using the equation

$$R = -\frac{N}{mt} \ln \frac{[HD]_\infty - [HD]_t}{[HD]_\infty - [HD]_0}$$

where N is the number of gaseous atoms, m zeolite weight (g), and $HD_{\infty,t,0}$ is concentration of HD molecules at the given time t (min).

RESULTS AND DISCUSSION

As the isotopic exchange reaction was measured at a temperature of 298 K, the γ-irradiation of zeolites was also carried out at 298 K to obtain defects sufficiently stable at this temperature. Therefore, H atoms which might be formed by the interaction of ejected electrons with H^+ ions necessarily recombined and were not detected.

ESR studies on the structure and stability of defects in γ-irradiated zeolites

HY zeolite. The ESR spectrum of zeolite in hydroxylated form (Fig. 1A) exhibits a wide signal of $\Delta H=38$ G with 7 hyperfine lines. An analogous spectrum has already been published with the parameters $g_1=2.002$, $c_1=7.5$ G, $g_2=2.005$, $c_2=8.0$ G, $g_3=2.045$ (6). It has been ascribed to skeletal Si-O-Si and Si-O-Al defects, the hyperfine splitting (hfs) corresponds to the interaction of the unpaired electron with the Al nucleus ($I_n=5/2$), the 7th line is coming from the anisotropic g factor. The assignement of the signal with the hfs to the Si-O-Al defects agrees with our interpretation. However, the presence of the localized Si-O-Si defects seems to be unprobable. Theoretical consideration supports the assumption of an unpaired electron delocalized over the lone pair orbitals of several skeletal oxygens denoted $(-O-)_n^\cdot$ in such a way that no hfs interaction of this electron with the Al nucleus is observed. Interaction of zeolite with hydrogen ($1.33.10^4$ Pa at 298 K, also for the zeolites described below) caused decrease of the complex signal and only a sharp low intensity signal close to the free electron value was retained. The latter signal corresponds probably to the ejected electron stabilized within the zeolite matrix and is found in all irradiated zeolites. Analogous behaviour of defects present in γ-irradiated silica containing Al impurities with respect to hydrogen was observed by Parijsky et al (9).

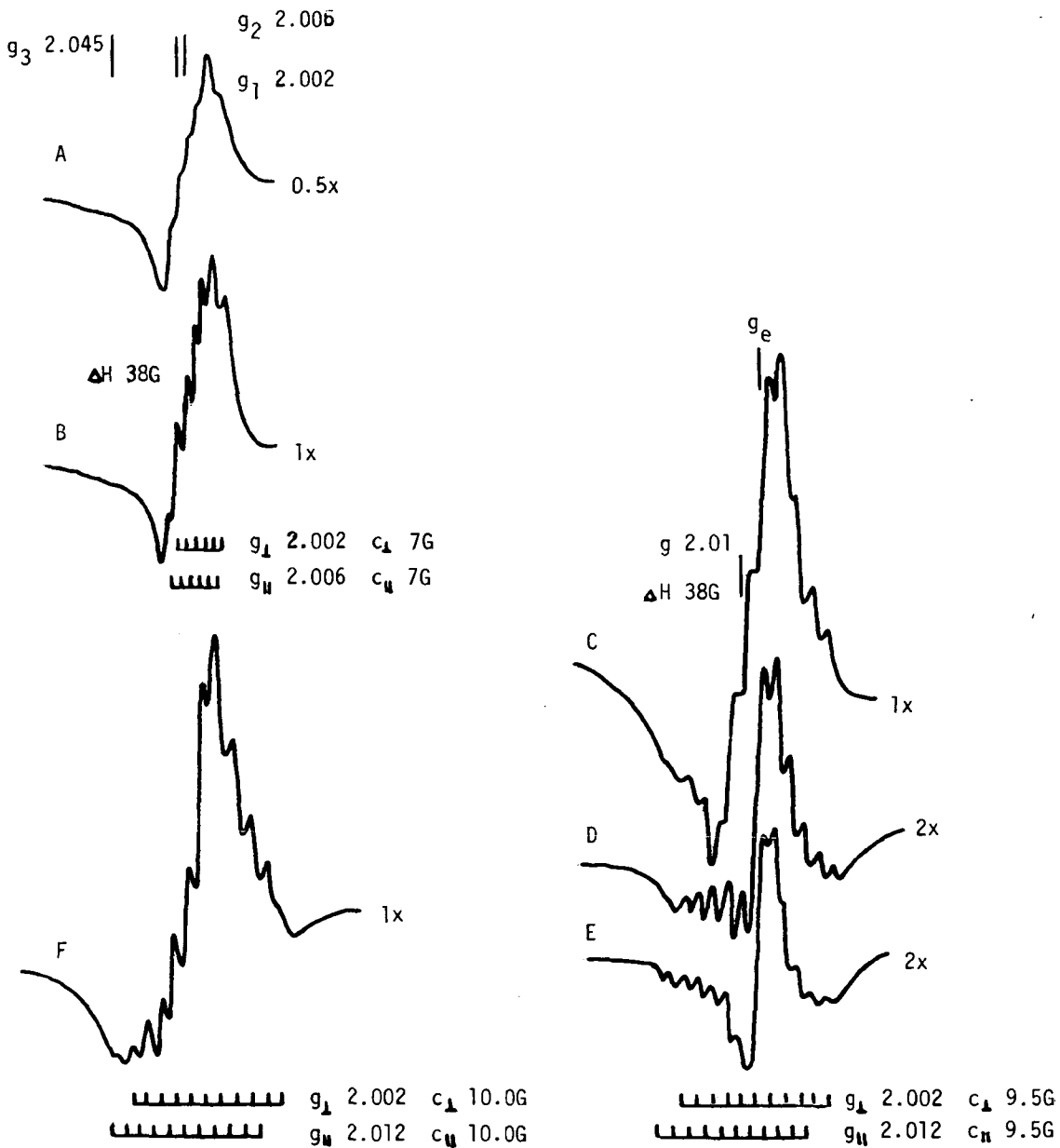HZSM-5 zeolite. The ESR spectrum of the hydroxylated zeolite exhibits a wide

Fig. 1. X-band ESR spectra of γ-irradiated zeolites at 298 K recorded at 80 K
A) HY, B) HZSM, C) AlHY, D) AlHY + $1.33.10^4$ Pa of H_2 for 15 minutes, E) AlHY +
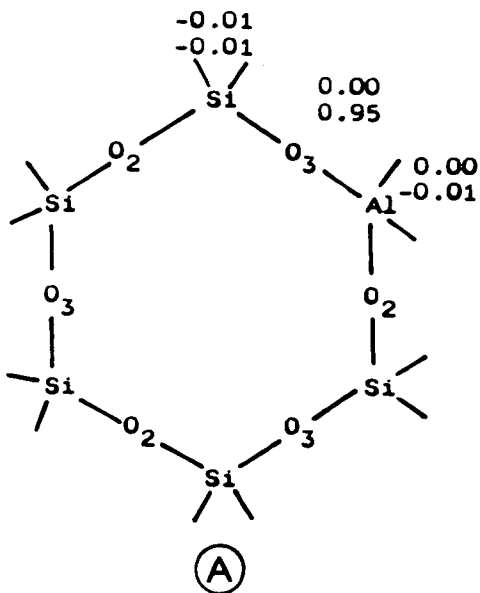+ $1.33.10^4$ Pa of H_2 for 24 hours, F) Al_xO_yHZSM-5

signal of $\Delta H = 38$ G with hyperfine splitting of 7 well resolved lines with the parameters given in Fig. 1B. This complex signal can be analogously attributed to the skeletal Si-O-Al and $(-O-)_n^{\cdot}$ defects. The better resolution of the hfs lines for HZSM compared to the HY zeolite may be a result of the low amount of Al in the skeleton of the HZSM-5 zeolite, as well as the higher degree of localization of defects arising from its lower structural symmetry. After treatment of the zeolite in hydrogen, the complex signal vanished and a signal close to g_e and a low intensity signal with 12 lines appeared. The latter signal is likely due to some additional defects on oxygen neighbouring extralattice Al (for comparison, see below) as such Al has been found in trace amounts in HZSM-5 zeolite using the IR spectra of pyridine adsorption (10).

AlHY zeolite. The zeolite with Al in the cationic sites (extralattice) and in the zeolite skeleton exhibits a broad signal with 12 hyperfine lines. The spectrum and its parameters are given in Fig. 1C. Treatment of the zeolite with hydrogen resulted in a decrease in the broad signal and in retention of the signal with 12 hfs lines and of the signal close to g_e (Fig. 1D). The intensity of the signal at g_e was constant, while the intensity of the splitted signal decreased slowly with time (Fig. 1E).
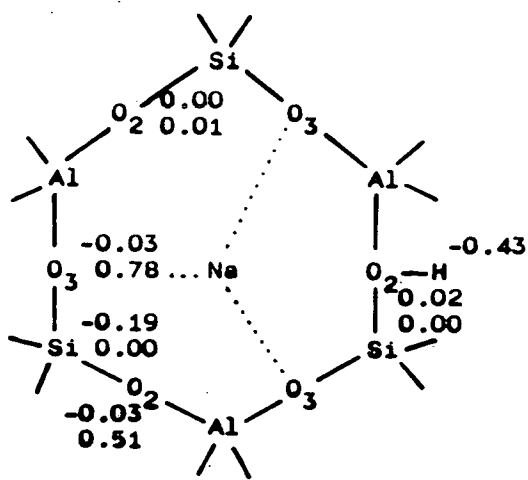
It is, therefore, evident that the spectrum of the irradiated zeolite consists of three particular signals: i) the sharp signal close to the g_e value (already mentioned), originating from the ejected electrons trapped within the zeolite material; ii) the signal with hfs of 12 lines (9.5 G) corresponding to an electron hole on an oxygen atom interacting with two Al atoms (12 lines being due to uniaxial symmetry of the g factor, cf. ref. 3, see Fig. 1C), iii) the broad signal which originates from the skeletal $(-O-)_n^{\cdot}$ defects already described for H-zeolites. Localized spin density on Si-O-Al defects is not present probably because of the easier formation of Al-O-Al defects in which one skeletal and one extralattice Al atom participate (cf. Fig. 2 model C). Then it is quite understandable that there is nearly zero probability of the creation of two defects close together.

Al$_x$O$_y$HZSM-5 zeolite. This zeolite with extralattice Al in the form of Al^{III} supported in the zeolite cavities again exhibits a complex broad signal with 12 well resolved hfs lines (10.0 G), indicating that, in addition to skeletal defects, the Al-O-Al defects are formed as a result of zeolite irradiation (Fig. 1F). Analogously as for the AlHY zeolite, the presence of hydrogen did not cancel the signal with 12 hfs lines. It can be assumed that in this zeolite, extralattice Al should exhibit various forms. It may possess a charge-balancing character or it may correspond to alumina species coordinate to the zeolite skeleton (cf. various species e.g. of Fe^{III} supported in zeolite (11)).
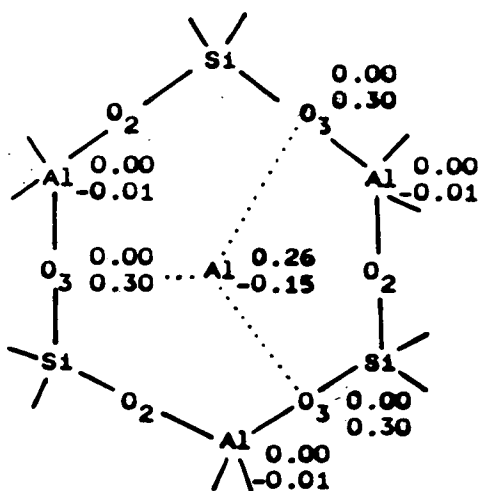
As for the stability of the V defects in γ-irradiated zeolites the ESR signal intensity of defects in HY zeolites was stable for several hours at 298 K, while that for AlHY and Al$_x$O$_y$HZSM-5 for several weeks. However, the signal intensity for HZSM-5 was slightly more stable than that for the HY zeolite. The total number of all

-0.01
-0.01

Si

0.00
0.95

O₂

O₃

0.00
-0.01

Si

Al

O₃

O₂

Si

Si

O₂

O₃

Si

(A)

Si

0.00
0.01

O₂

O₃

Al

Al

-0.03
0.78 ... Na

O₃

-0.43

O₂—H
0.02
0.00

-0.19
Si 0.00

Si

O₂

O₃

-0.03
0.51

Al

(B)

Si

0.00
0.30

O₂

O₃

0.00
-0.01

Al

Al

0.00
-0.01

O₃ 0.00
0.30

Al 0.26
-0.15

O₂

Si

O₂

O₃ 0.00
0.30

Al

0.00
-0.01

(C)

Fig. 2. Schematic depiction of the clusters studied with indication of spin
densities (higher or equal than 0.01) in the s atomic orbital (upper value) ·and
in the p atomic orbital (lower value) on individual atoms. Positive values
stand for α spin densities and negative for β spin densities.

defects is of the order of 10^{19}, i.e. it is substantially lower than the number of sites available for their formation. This is understandable from the point of view of the low stability of these defects as well as of the ejected electrons trapped in the zeolite material. The number of the individual defects is difficult to estimate because of the signal overlap.

Model quantum chemical calculations on defects in γ-irradiated zeolites

Localization of an unpaired electron in the H- and Al-forms of faujasites was also investigated by means of model quantum chemical calculations. The standard version of the UHF CNDO/2 method (12) with an s,p base for Si and Al atoms was employed (13) in the calculations. The zeolites were then modelled using the following cluster models: i) The $Si_5AlO_6(OH)_{12}^-$ cluster, representing a six-member zeolitic window facing the large cavity (Fig. 2A); ii) The $Si_3Al_3O_6(OH)_{12}NaH^\cdot$ cluster, depicting the same window with the Na cation coordinated in the S_I cationic position and the skeletal hydroxyl group formed by the O_2 type of oxygen (Fig. 2B); iii) The $Si_3Al_3O_6(OH)_{12}Al^\cdot$ cluster, modelling the same window with an Al cation again situated in the cationic position (Fig. 2C). The models were terminated by H atoms and their geometry characteristics were taken from X-ray data (14).

The values of α- and β-spin densities calculated for the clusters studied are listed in Fig. 2. From these values it follows that: i) If no cations or protons are bonded to the zeolitic skeleton, the unpaired electron is mainly located in the lone pair orbital of the skeletal oxygen atom bonded to the Al and Si atoms. The remaining part of the α-spin density is delocalized over the whole cluster. Only a very small amount of β-spin density is also situated on the Si and Al atoms adjacent to the O atom bearing the major part of the unpaired electron. ii) If, in addition to the Na cation, a proton is bonded to the skeletal O_2 atom, the α-spin density is again located in the lone pair orbital of the skeletal O atoms. Simultaneously, however, a relatively large amount of the β-spin density is found on the H atom forming this OH group. iii) When an Al cation is coordinated in the cationic position, the unpaired electron is mainly located on the Al cation and in the lone pair orbitals of the O_3 atoms coordinating this cation. A very small amount of the β-spin density is also situated on the skeletal Al atoms.

Catalytic activity of defects in the γ-irradiated zeolites in D_2-H_2 exchange

The activity of irradiated zeolites can be ascribed to the defects formed by their irradiation, as original zeolites listed in Table 2 did not exhibit any D_2-H_2 exchange activity at 298 K. While the defects formed in the HY zeolite exhibit relatively low activity which completely disappears after the zeolite treatment in hydrogen at low pressure, the zeolites with extralattice Al possess substantially higher and very stable activity. The activity of the Al_xO_yHZSM-5 zeolite was stable even after exposure of the zeolite to 10^5 Pa of hydrogen for 1 hour. The higher and stable activity of ZSM-5 compared to the Y zeolites can be accounted for in terms of

Table 2

Rate of the D_2-H_2 exchange on irradiated zeolites at 298 K

Irradiated zeolite	HY	AlHY	HZSM-5	Al_xO_yHZSM-5
$R.10^{-19}$ atom/min.g	0.2	3.9	6.1	19.8
$R^a.10^{-19}$ atom/min.g	0	2.4	6.1	19.8

[a] after zeolite treatment in 4.10^{19} molecules of hydrogen at 298 K for 1 hour

the structural differences together with the presence of some extralattice Al, which is always present in small amounts in the HZSM-5 zeolite (see above and ref. 10).

CONCLUSIONS

The results given indicate that γ-irradiation of zeolites may produce electron holes located at various sites of the zeolite structure, depending on the type of zeolite. With H-zeolites not containing extralattice Al, electron holes are mainly localized in lone pair orbitals of the skeletal oxygen atoms. A small amount of spin density is also situated on the adjacent Al atom. Therefore, they correspond to the skeletal Si-O-Al and $(-O-)_n$ defects. On the other hand, if the zeolite contains extralattice Al species (either in the cationic form or supported in the zeolite cavities) then, in addition to the Si-O-Al and $(-O-)_n$ defects, it exhibits an electron hole on an oxygen atom neighbouring two Al atoms (Al-O-Al). These defects seem to be formed by a skeletal oxygen bonded to one skeletal and one extralattice Al atom. Moreover, a substantially larger amount of spin density appears to be located on the Al atoms compared to the Al-O-Si defects. Nevertheless, the presence of Al-O-Al defects formed by two extralattice Al atoms cannot be fully excluded, but their existence seems to be less probable as they have never been observed in pure γ-irradiated aluminas. Much higher stability of the Al-O-Al defects compared to the remaining observed defects in a hydrogen atmosphere is understandable, as the latter defects are capable of capturing hydrogen and formed OH groups. On the contrary, supposing that the Al-O-Al defects consisted of a skeletal oxygen sharing one skeletal and one extralattice Al atom, then the lone pair orbitals of this oxygen are saturated by the extralattice Al and, therefore, it can bond an additional H atom only with difficulty.

In this way it is also possible to explain different activities of γ-irradiated H- and Al-zeolites in D_2-H_2 exchange. All irradiated zeolites exhibit very high activity even at a low temperature at which the original zeolites are quite inactive. Particularly the presence of Al-O-Al defects substantially increases and stabilizes the zeolite activity. The reactivity of the Al-O-Al, Al-O-Si and $(-O-)_n$ defects in the

D_2-H_2 exchange cannot be simply compared, as the latter two defects are quickly annihilated by the interaction with hydrogen. For Si-0-Al defects, this process seems to be consistent with the following scheme

$$\overset{\cdot}{Si\text{-}O\text{-}Al} + H_2 = Si\text{-}\underset{H}{\overset{|}{O}}\text{-}Al + H^+$$
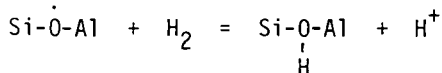
explaining both annihilation of the Si-0-Al defects and limited D_2-H_2 exchange. The delocalized $(\text{-O-})_n^{\cdot}$ skeletal defects are probably eliminated in a similar way.

REFERENCES

1. Stamires, D.N. and Turkevich, J., J, Amer. Chem. Soc. 86, 757 (1964).
2. Wang, K.M. and Lunsford ,J.H., J. Catal. 24, 262 (1972).
3. Vedrine, J.C., Abou-Kais, A., Massardier, J. and Dalmai-Imelik G., J. Catal. 29, 120 (1973).
4. Vedrine, J.C. and Nacchache, C., J. Phys. Chem. 77, 1606 (1973).
5. Abou-Kais, A., Vedrine, J.C., Massardier, J. and Dalmai-Imelik, G., J. Chem. Soc., Faraday Trans. 1, 70, 1039 (1974) and refs. therein.
6. Abou-Kais, A., Vedrine, J.C. and Massardier, J., J. Chem. Soc., Faraday Trans. 1, 71, 1697 (1974).
7. Garibov, A.A. and Melikadze, M.M., Zhur. Fiz. Chim. 54, 2607 (1980).
8. Gupta, N.M., Kamble, V.S. and Iyer ,R.M., J. Catal. 66, 101 (1980).
9. Parijsky, G.B., Mischenko, Yu.A. and Kazansky, V.B., Kin. Katal. 6, 625 (1965).
10. Novakova, J., Kubelkova, L., Habersberger, K. and Dolejsek, Z., J. Chem. Soc., Faraday Trans. 1, 80, 1457 (1984).
11. Novakova, J., Kubelkova, L., Wichterlova, B., Juska, T. and Dolejsek ,Z., Zeolites 2, 17 (1982).
12. Pople, J.A. and Beveridge, D.L. ,Approximate Molecular Orbital Theory, Mc Graw-Hill, New York, 1970.
13. Beran, S. and Dubsky, J., J. Phys. Chem., 83, 2538 (1979).
14. Eulenberger, G.R., Schoemaker, D.P. and Keil, J.G., J. Phys. Chem. 71, 1812 (1976).